

Arrestins function in cAR1 GPCR-mediated signaling and cAR1 internalization in the development of *Dictyostelium discoideum*

Xiumei Cao^{a,*}, Jianshe Yan^{a,b,*}, Shi Shu^c, Joseph A. Brzostowski^d, and Tian Jin^b

^aShanghai Institute of Immunology, Shanghai Jiao Tong University School of Medicine, Shanghai 200025, China; ^bChemotaxis Signal Section, Laboratory of Immunogenetics, and ^dLaboratory of Immunogenetics Imaging Facility, National Institute of Allergy and Infectious Diseases, National Institutes of Health, Rockville, MD 20852; ^cLaboratory of Cell Biology, National Heart, Lung, and Blood Institute, National Institutes of Health, Bethesda, MD 20892

ABSTRACT Oscillation of chemical signals is a common biological phenomenon, but its regulation is poorly understood. At the aggregation stage of *Dictyostelium discoideum* development, the chemoattractant cAMP is synthesized and released at 6-min intervals, directing cell migration. Although the G protein-coupled cAMP receptor cAR1 and ERK2 are both implicated in regulating the oscillation, the signaling circuit remains unknown. Here we report that *D. discoideum* arrestins regulate the frequency of cAMP oscillation and may link cAR1 signaling to oscillatory ERK2 activity. Cells lacking arrestins (*adcB*⁻) display cAMP oscillations during the aggregation stage that are twice as frequent as for wild-type cells. The *adcB*⁻ cells also have a shorter period of transient ERK2 activity and precociously reactivate ERK2 in response to cAMP stimulation. We show that arrestin domain-containing protein C (AdcC) associates with ERK2 and that activation of cAR1 promotes the transient membrane recruitment of AdcC and interaction with cAR1, indicating that arrestins function in cAR1-controlled periodic ERK2 activation and oscillatory cAMP signaling in the aggregation stage of *D. discoideum* development. In addition, ligand-induced cAR1 internalization is compromised in *adcB*⁻ cells, suggesting that arrestins are involved in elimination of high-affinity cAR1 receptors from cell surface after the aggregation stage of multicellular development.

Monitoring Editor

Peter Van Haastert
University of Groningen

Received: Mar 27, 2014

Revised: Aug 5, 2014

Accepted: Aug 10, 2014

INTRODUCTION

Coordinated cell movement is a biological process essential for the multicellular development of most organisms, and this process requires exquisitely controlled cell-cell signaling. Oscillatory signaling is one basic mode of cell-cell communication in many biological systems (Goldbeter, 2002; Gregor *et al.*, 2010). Oscillatory chemical signaling encodes information not only in chemical structure and

concentration, but also in the frequency of oscillations (Goldbeter, 2002). The molecular mechanisms responsible for oscillations are not well understood. Chemoattractant signaling in the social amoeba *Dictyostelium discoideum* is one of the best known examples of oscillatory cell-cell signaling that organizes cooperative cell movement (Gerisch *et al.*, 1975; Tomchik and Devreotes, 1981; Maeda *et al.*, 2004). During the initial stages of development, *D. discoideum* cells spontaneously emit pulses of the chemoattractant cAMP. Centers of cAMP oscillations self-organize, and surrounding cells respond by producing and releasing additional cAMP and at the same time migrate toward the center of cAMP pulses (Gerisch *et al.*, 1975; Tomchik and Devreotes, 1981). Aggregating *D. discoideum* cells use the G protein-coupled receptor (GPCR) cAMP receptor 1 (cAR1) to sense extracellular cAMP, and the cells respond to the cAMP stimuli by propagating cAMP waves with a period of ~6 min (Parent and Devreotes, 1996; Maeda *et al.*, 2004).

Oscillatory cAMP signaling is controlled by a cAR1-mediated signaling circuit that regulates the activation and inhibition of adenylyl

This article was published online ahead of print in MBoC in Press (<http://www.molbiolcell.org/cgi/doi/10.1091/mbc.E14-03-0834>) on August 20, 2014.

*These authors contributed equally.

Address correspondence to: Tian Jin (tjin@niaid.nih.gov), Jianshe Yan (yanjianshe@sjtu.edu.cn).

Abbreviations used: Adc, arrestin domain-containing protein; cAR, cAMP receptor; ERK, extracellular signal-regulated kinase; GPCR, G protein-coupled receptor.

© 2014 Cao, Yan, *et al.* This article is distributed by The American Society for Cell Biology under license from the author(s). Two months after publication it is available to the public under an Attribution-NonCommercial-Share Alike 3.0 Unported Creative Commons License (<http://creativecommons.org/licenses/by-nc-sa/3.0>).

"ASCB[®]," "The American Society for Cell Biology[®]," and "Molecular Biology of the Cell[®]" are registered trademarks of The American Society of Cell Biology.

cyclase (ACA), as well as the cyclical degradation of both intracellular and extracellular cAMP (Kriebel *et al.*, 2003; Maeda *et al.*, 2004; Bader *et al.*, 2007). The cAR1-controlled pathway leading to ACA activation involves the dissociation of heterotrimeric G protein subunits G α 2 and G β γ , which in turn activate many transient responses, including the activation of ACA (Parent and Devreotes, 1996; Kriebel *et al.*, 2003). cAR1 also controls the activity of the cAMP-specific intracellular phosphodiesterase RegA, and hence intracellular cAMP degradation, via periodic regulation of extracellular signal-regulated kinase 2 (ERK2) signaling (Segall *et al.*, 1995; Maeda *et al.*, 2004). On cAMP stimulation, an ERK2 kinase is activated, and an ERK2 phosphatase is believed to be inactivated, resulting in transient ERK2 phosphorylation and activation (Maeda *et al.*, 1996, 2004; Brzostowski and Kimmel, 2006). A previous study indicated that cAMP-controlled ERK2 activation oscillates in synchrony with extracellular cAMP waves (Maeda *et al.*, 2004). However, the molecular components that are involved in cAR1 GPCR-controlled ERK2 activation have not been completely identified, and the mechanisms underlying the regulation of cAMP waves are not clear.

β -Arrestins are an evolutionarily conserved family of proteins that serve as mediators of GPCR-controlled ERK2 signaling in mammalian cells (Lefkowitz and Shenoy, 2005; DeFea, 2011). GPCRs constitute a large family of receptors that enable eukaryotic cells to sense various extracellular signals, such as hormones, neurotransmitters, chemokines, light, and odorants (Lefkowitz and Shenoy, 2005; DeFea, 2011). On ligand binding, a GPCR changes its conformation and triggers the dissociation of heterotrimeric G proteins into G α and G β γ subunits, which in turn activate multiple signaling pathways (Lefkowitz and Shenoy, 2005). Activation of the GPCRs also leads to receptor phosphorylation by G protein-coupled receptor kinases (GRKs) and induces translocation of cytosolic β -arrestins to the plasma membrane to form a complex with these GPCRs (Brzostowski and Kimmel, 2001; Lefkowitz and Shenoy, 2005; DeFea, 2011; Shukla *et al.*, 2013). The translocated β -arrestins affect GPCR signaling by performing multiple functions. First, β -arrestins block the coupling between GPCR and G proteins, which results in the desensitization of GPCRs (Lefkowitz and Shenoy, 2005; DeFea, 2011; Shenoy and Lefkowitz, 2011). Second, β -arrestins mediate GPCR endocytosis via clathrin-coated pits, leading to the internalization of GPCRs from the cell surface (Lefkowitz and Shenoy, 2005; Shenoy and Lefkowitz, 2011). Third, β -arrestins mediate downstream signaling cascades, including mitogen-activated protein kinase (MAPK) ERK2 signaling, by controlling the activity of kinases, such as Src and MAPK, and other enzymes (DeFea, 2011; Shenoy and Lefkowitz, 2011). These functions of β -arrestins have been well-studied for several GPCRs, such as β -adrenergic receptors (Lohse *et al.*, 1990; Granier *et al.*, 2007; Shenoy and Lefkowitz, 2011). Recently β -arrestins have been implicated as regulators of chemokine GPCR-mediated chemotaxis in mammalian cells (DeFea, 2007).

Eukaryotic arrestins split into two major clades: the more ancient, and recently identified, alpha family and the visual/beta family (Alvarez, 2008). Six *D. discoideum* genes, *adcA–E*, have been found to encode proteins containing arrestin-homology domains (Aubry *et al.*, 2009). A previous study reported that arrestin domain-containing protein A (AdcA) plays a role in the formation of early endosomes (Guetta *et al.*, 2010). It is not clear whether or which arrestin-like protein functions in GPCR-mediated signaling and/or the internalization of GPCRs in *D. discoideum*. Here we report the roles of AdcC in cAR1-mediated cAMP signaling in *D. discoideum*. Our data indicate that cAR1-mediated arrestin function regulates the period of transient ERK2 activation that controls the frequency of cAMP oscillations at the aggregation stage of *D. discoideum* develop-

ment. In addition, we show that cAMP-induced cAR1 internalization is compromised in cells lacking AdcB and AdcC, suggesting that arrestins-like proteins are involved in ligand-induced cAR1 internalization in *D. discoideum*.

RESULTS

Arrestins play roles in development of *D. discoideum*

We investigated the functions of *adcB* (gene ID, DDB_G0274395) and *adcC* (gene ID, DDB_G0271022) in the development of *D. discoideum*. The proteins encoded by *adcB* and *adcC* have a similar domain structure and share high similarity in overall amino acid sequence (Supplemental Figure S1). We first generated individual *adcB*⁻ and *adcC*⁻ cells (*adcB*⁻ and *adcC*⁻, respectively) through homologous recombination. We also made *adcB*⁻*adcC*⁻ double-null cells by using the Cre-loxP system, reasoning that these proteins may have overlapping functions due to their similarity. Each of the null mutants was confirmed by PCR analysis (Supplemental Figure S2).

To reveal the potential roles of these genes in the development of *D. discoideum*, we analyzed the developmental phenotypes of *adcB*⁻, *adcC*⁻, and *adcB*⁻*adcC*⁻ cells on bacterial lawns (Figure 1A and Supplemental Figure S3) and on nonnutrient agar (Figure 1C). Whereas *adcB*⁻ and *adcC*⁻ cells displayed a wild-type-like phenotype, *adcB*⁻*adcC*⁻ cells were unable to form a normal number of mounds in each plaque (Figure 1, A and B) and failed to aggregate by 5 h, but they eventually formed smaller aggregates at 10 h on nonnutrient agar (Figure 1C). The developmental phenotype was partially rescued by expressing either yellow fluorescent protein (YFP)-tagged AdcB or AdcC (Figure 1, A and B), indicating that either AdcB or AdcC is required for proper development of *D. discoideum* and that both AdcB-YFP and AdcC-YFP are functional.

To determine whether AdcB and AdcC play roles in chemotaxis of *D. discoideum*, we performed the EZ-TAXIScan chemotaxis assay to compare the migration of the wild-type and *adcB*⁻*adcC*⁻ cells to a cAMP gradient ranging from 0 to 1 μ M and found that *adcB*⁻*adcC*⁻ cells exhibited normal chemotactic behaviors (Supplemental Movies S1 and S2), indicating that AdcB and AdcC do not directly regulate chemotaxis in *D. discoideum*.

AdcC translocates to the cell membrane upon activation of cAR1

To test whether activation of cAR1 GPCR controls the functions of arrestins, we observed the cellular localization of AdcC-YFP upon cAMP stimulation (Figure 2). Before stimulation, AdcC-YFP was localized in the cytosol of the cells. On cAMP stimulation, AdcC-YFP transiently translocated to a region proximal to the plasma membrane in *adcC*⁻ cells expressing AdcC-YFP (*adcC*⁻/AdcC-YFP; Figure 2, A and B); however, cAMP-induced translocation was not observed for AdcB-YFP, indicating that these proteins do not have completely redundant functions (Supplemental Figure S4). The transient relocalization of certain proteins to the intracellular face of the plasma membrane requires actin reorganization (Yan *et al.*, 2012). To test whether actin dynamics is required for the translocation of AdcC, we pretreated cells with latrunculin B, an inhibitor of actin polymerization. On stimulation, no effect was observed on AdcC-YFP dynamics in the presence of latrunculin B (Figure 2, C and D). In addition, cAMP-induced membrane recruitment of AdcC-YFP occurred in cells lacking functional heterotrimeric G-proteins (g β ⁻/AdcC-YFP; Figure 2, E and F) but not in RI9 cells, which lack the cAMP receptors cAR1 and cAR3 (Insall *et al.*, 1994; Figure 2, G and H), indicating that activation of cAR1 triggers G protein-independent membrane recruitment of AdcC-YFP.

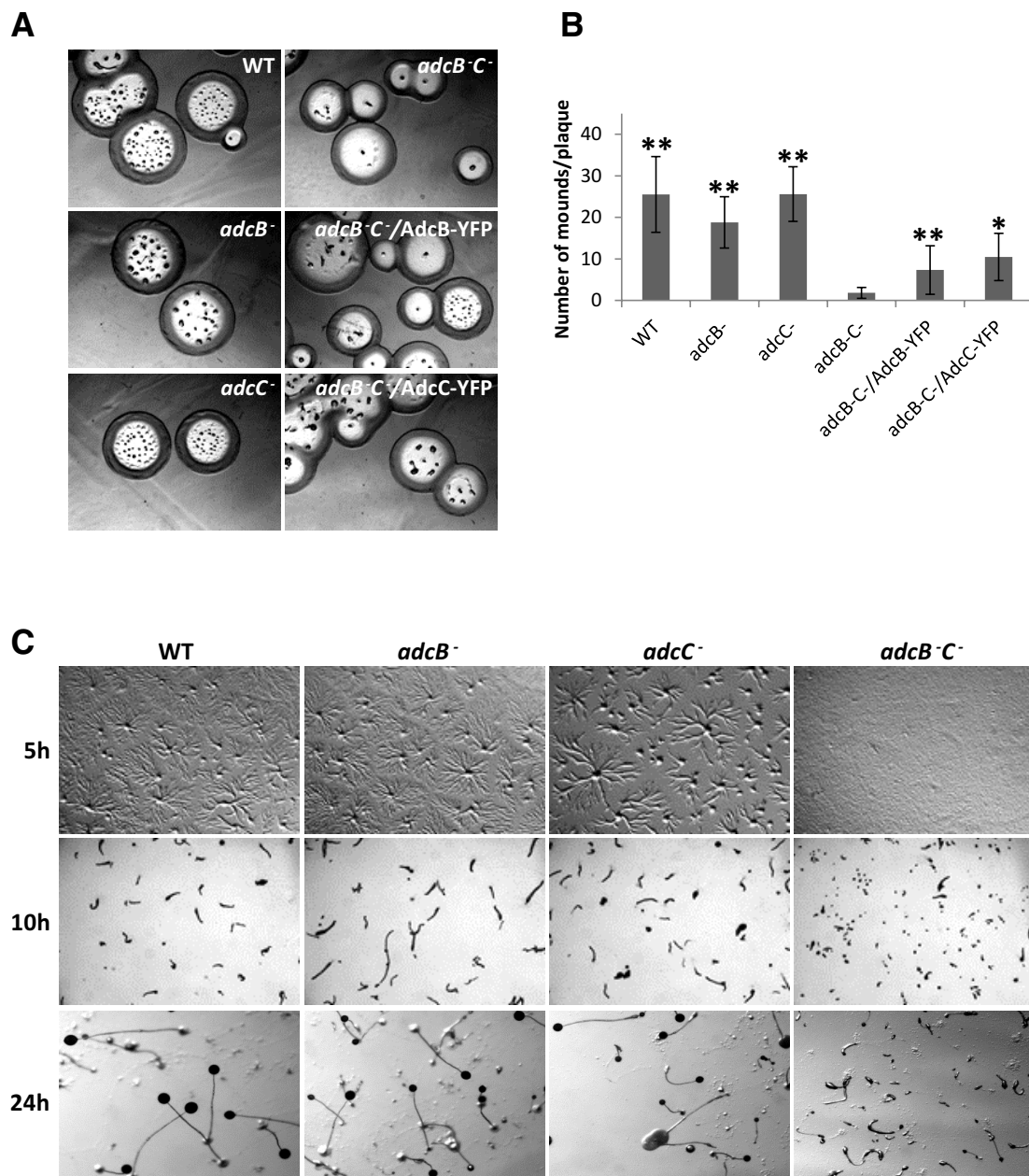


FIGURE 1: Arrestin-like proteins function in the development of *D. discoideum*. (A) Development of arrestin null cells on bacterial lawns. Wild-type, *adcB*^{-/-}, *adcC*^{-/-}, *adcB*^{-/-}*C*^{-/-}, and *adcB*^{-/-}*C*^{-/-} cells expressing AdcB-YFP or AdcC-YFP were grown in association with *K. aerogenes* at 22°C. Photographs were taken after 5 d. (B) The number of mounds in plaques formed by cells was counted and graphed. Means ($n = 4-6$) and SDs are shown. Statistical significance was assessed by *t* test, * $p < 0.05$ and ** $p < 0.01$. (C) Development of arrestin null cells on nonnutrient agar. Arrestin-null cells were plated on nonnutrient agar to initiate starvation and the developmental program. Images were captured at the indicated times to show aggregation (5 h), slug (10 h), and fruiting body (24 h) stages.

Activation of cAR1 receptors not only triggers G protein-independent signaling events but also induces dissociation of heterotrimeric G protein into G α 2 and G β γ subunits, which regulate multiple signaling transduction pathways controlling the actin cytoskeleton (Janetopoulos *et al.*, 2001). The cAR1/G α 2G β γ machinery regulates a pathway involving the small G protein Ras, phosphoinositide 3-kinase, and phosphatase and tensin homologue to control phosphatidylinositol (3,4,5)-trisphosphate (PIP₃) during chemotaxis (Parent *et al.*, 1998; Funamoto *et al.*, 2001, 2002; Iijima and Devreotes, 2002; Sasaki *et al.*, 2004). The changes

in the level of PIP₃ were monitored *in vivo* by the PIP₃-binding fluorescent probe PH_{Crac}-GFP (Parent *et al.*, 1998; Xu *et al.*, 2005). We found that cAR1-mediated PIP₃ responses to cAMP stimulation was normal in *adcB*^{-/-} cells as monitored by the transient translocation of PH_{Crac}-GFP to the plasma membrane (Figure 2, I and J). Thus activation of cAR1 induces membrane recruitment of AdcC, but the arrestins AdcB and AdcC do not play essential roles in cAR1/G α 2G β γ -controlled pathways, many of which are essential for chemotaxis of *D. discoideum*, which is consistent with our observations.

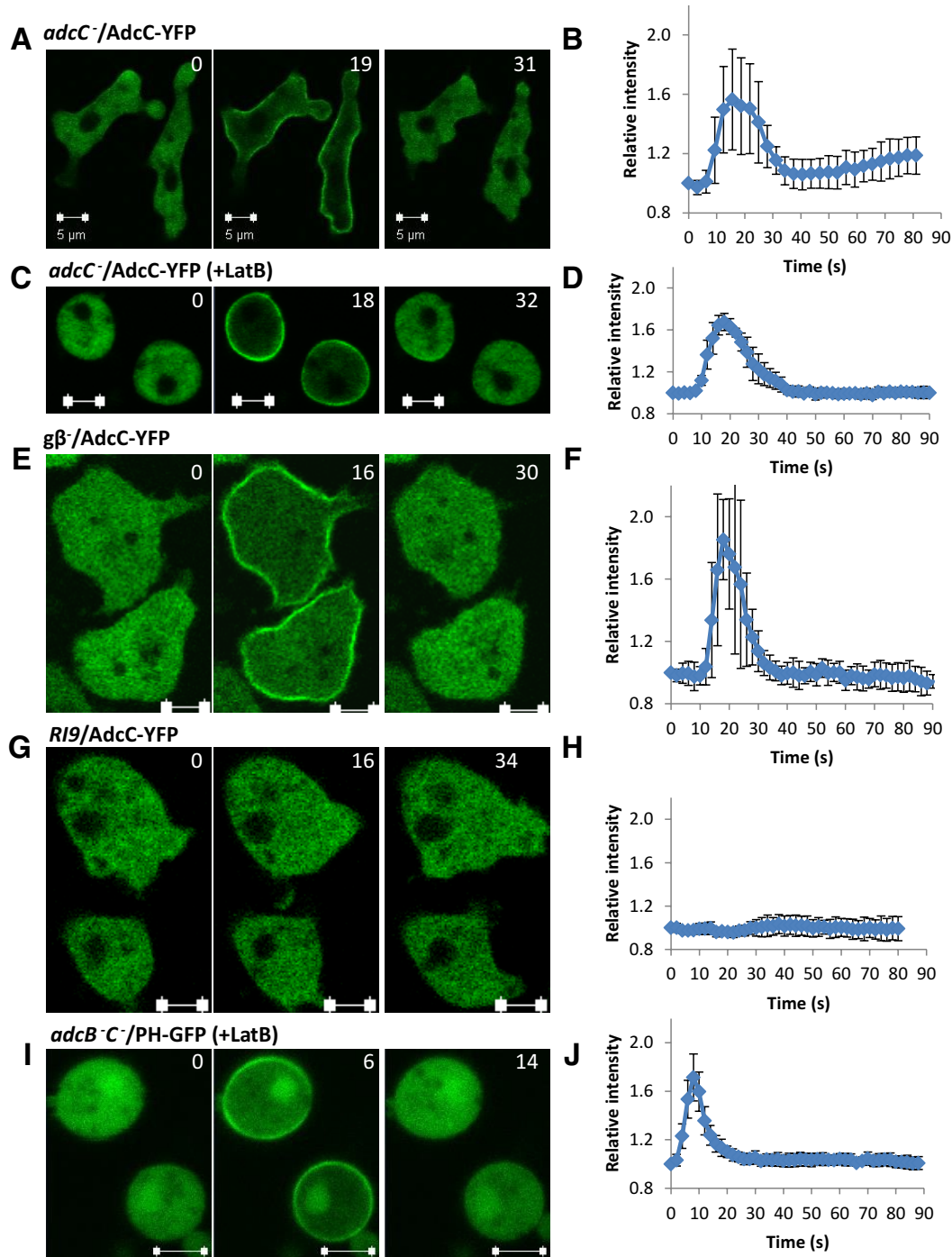


FIGURE 2: AdcC transiently translocates from the cytosol to the cell membrane in an actin- and G protein-independent manner upon stimulation. (A) AdcC-YFP transiently associates with plasma membrane upon cAMP stimulation. *adcC*⁻ cells expressing AdcC-YFP were stimulated with 10 μM cAMP. (B) Kinetics of the time course. Means (*n* = 7) and SDs are shown. (C, D) cAMP-induced AdcC membrane translocation does not depend on the actin cytoskeleton. *adcC*⁻ cells expressing AdcC-YFP were treated with latrunculin B to depolarize the actin cytoskeleton and stimulated with cAMP. Means (*n* = 6) and SDs are shown. (E, F) cAMP-induced AdcC membrane translocation does not require Gβ. Translocation of AdcC-YFP in *gβ*⁻ cells was monitored by time-lapse confocal microscopy after cAMP stimulation. Means (*n* = 6) and SDs are shown. (G, H) cAMP-induced AdcC membrane translocation requires cAR1 signaling. Temporal changes in the levels of AdcC-YFP at the plasma membrane are shown as a time course for RI9 (*car1*/*car3*) cells expressing AdcC-YFP. Means (*n* = 6) and SDs are shown. (I, J) cAMP-induced PH_{CRAC}-GFP translocation appears normal in arrestin-null cells. *adcB*⁻*C*⁻ cells expressing PH_{CRAC}-GFP were treated with latrunculin B to depolarize the actin cytoskeleton and stimulated with cAMP. The levels of PH_{CRAC}-GFP at the plasma membrane are shown as a time course. Means (*n* = 6) and SDs are shown. Scale bar, 5 μm. In A and B, images were captured at 3.1-s intervals, and in B–J, images were captured at 2-s intervals; selected time points are shown.

AdcC associates with the GPCR cAR1

As with mammalian GPCRs, cAR1 is phosphorylated upon ligand stimulation (Klein *et al.*, 1987; Hereld *et al.*, 1994). Our observation that AdcC transiently localizes to the plasma membrane prompted us to examine the potential phosphorylation-dependent association between cAR1 and AdcC by performing coimmunoprecipitation analyses on extracts from cells coexpressing AdcC-mCherry and cAR1-YFP, cm1234-YFP, a mutant cAR1 that lacks all ligand-induced phosphorylation sites in its C-terminal cytoplasmic domain (Hereld *et al.*, 1994), or the YFP-tag control in RI9 (*car1⁻/car3⁻*) cells (Insall *et al.*, 1994; Supplemental Figure S5). In addition, RFP-ERK2 was coexpressed with cAR1-YFP in the RI9 strain to determine whether it associates with the receptor. In unstimulated cells, we found that AdcC-mCherry coimmunoprecipitated with cAR1-YFP and cm1234-YFP but not with the YFP-tag control. In addition, RFP-ERK2 did not coimmunoprecipitate with cAR1-YFP (Figure 3A). On cAMP stimulation, a 2.5-fold increase in AdcC-mCherry was observed in coimmunoprecipitates with cAR1-YFP but not with cm1234-YFP (Figure 3, A and B). Our results suggest that AdcC can increase its association with the receptor in a ligand-dependent manner that requires the presence of phosphorylatable residues at cAR1's C-terminus.

We further examined the association between cAR1 and AdcC upon uniform cAMP stimulation of live cells. Cells coexpressing either cAR1-YFP and AdcC-mCherry or cm1234-YFP and AdcC-mCherry were imaged by confocal time-lapse microscopy before and after stimulation. As expected, cAMP stimulation induced clear membrane translocation of AdcC-mCherry in the presence of cAR1 (Figure 3, C and F) but not in the control RI9 (*car1⁻/car3⁻*) cells expressing AdcC-mCherry alone (Figure 3, E and H). Of note, AdcC-mCherry membrane translocation occurred specifically in cells with detectable cAR1-YFP but not in cells expressing AdcC-mCherry alone in the same imaging field (Figure 3, C and D). Of interest, cAMP stimulation also triggered membrane translocation of AdcC-mCherry in cells expressing only cm1234 mutant receptors (Figure 3, D and G). Taken together, our results suggest that cAMP-induced membrane translocation requires cAR1; however, membrane recruitment of AdcC does not depend on receptor phosphorylation at its C-terminus, indicating that, in addition to cAMP-induced interaction between AdcC and phosphorylated cAR1, other cAR1 signaling events also play a role in membrane translocation of AdcC in live cells.

AdcC associates with ERK2 and contributes to cAMP-mediated ERK2 signaling

To reveal the potential molecular mechanism of AdcC function, we attempted to identify proteins that associate with AdcC (Supplemental Figure S6). AdcC-YFP-TAP expressed in *adcC⁻* cells was partially purified from lysates using anti-GFP antibodies coupled to beads, and elutes were subjected to SDS gel electrophoresis and mass spectrometry analysis; the YFP-TAP tag expressed in *adcC⁻* cells was used as a control. Our analysis identified possible candidates, including clathrin and E3 ubiquitin-protein ligase, which are known to interact with β -arrestin (Krupnick *et al.*, 1997; Shenoy *et al.*, 2001), indicating that this approach could reveal AdcC-associating proteins. ERK2 was also among the possible candidates (Supplemental Figure S6B). To confirm the association between AdcC and ERK2, we immunoprecipitated AdcC-YFP from lysates of cells coexpressing AdcC-YFP and RFP-ERK2 or YFP alone and RFP-ERK2 using an anti-GFP antibody. We found that RFP-ERK2 was detected only in lysates containing AdcC-YFP but not YFP alone (control; Figure 4A). In a reciprocal experiment, RFP-ERK2 but not RFP alone pulled down AdcC-YFP

(Supplemental Figure S6C), indicating the association between AdcC and ERK2.

We then examined the role of AdcC in cAR1-induced ERK2 signaling. cAMP stimulation induces transient phosphorylation of ERK2 on threonine and tyrosine residues in the activation loop of the protein (Gutkind, 2000). The level of ERK2 phosphorylation represents ERK2 activation, which can be monitored by Western blotting using anti-phospho-threonine/tyrosine ERK2 antibodies (Kosaka and Pears, 1997). Using this assay, we compared the temporal kinetics of cAMP-induced ERK2 phosphorylation in wild-type, *adcB⁻C⁻*, and *adcB⁻C⁻* cells expressing AdcC-YFP (*adcB⁻C⁻/AdcC-YFP*) in response to 1 μ M (Figure 4, B and D) or 50 μ M cAMP stimulation (Figure 4, C and E). Cells were differentiated to the chemotactic stage of development by providing exogenous cAMP pulses in culture. The level of native cAR1 was determined to be the same in wild-type and *adcB⁻C⁻* cells after development (Supplemental Figure S7A). In all cases after stimulation, pERK2 levels increased rapidly and peaked by 1 min, and the total level of ERK2 remained unchanged during the rapid time course, indicating that neither AdcB nor AdcC is required for ERK2 activation (Figure 4B). Total ERK2 levels were found to be similar in all cell lines tested when probed on the same blot (Supplemental Figure S7B). In response to 1 μ M cAMP stimulation, ERK2 phosphorylation returned to a prestimulus level in 3 min in *adcB⁻C⁻* cells and in 5 min in wild-type cells (Figure 4, B and D). On stimulation with a saturating dose of cAMP (50 μ M), ERK2 phosphorylation was prolonged and remained elevated for >8 min in wild-type cells. In contrast, the ERK2 phosphorylation in *adcB⁻C⁻* cells clearly dropped to almost a prestimulus level by 3 min before increasing again (Figure 4, C and E). Furthermore, this biphasic phenotype of *adcB⁻C⁻* cells could be rescued by AdcC-YFP (Figure 4, B–E). These results support the notion that activation of cAR1 controls a pathway responsible for ERK2 phosphorylation/activation and another that regulates its dephosphorylation/deactivation (Brzostowski and Kimmel, 2006). Of importance, our study suggests that AdcC and ERK 2 associate, and, presumably as a result of this association, cAR1 prolongs ERK2 activity and thus regulates the periodicity of ERK2 signaling. In *adcB⁻* and *adcC⁻* mutant cells, we did not detect any defect in cAR1-induced ERK2 phosphorylation (Supplemental Figure S8), suggesting that either AdcC or AdcB may function to regulate ERK2 signaling.

Arrestins play a role in controlling oscillations of cAMP signaling

A previous study showed that ERK2 activity oscillates in phase with extracellular cAMP waves during specific stages of development of *D. discoideum* (Maeda *et al.*, 2004). To test whether arrestins play a role in cAR1-controlled oscillations of cAMP signaling, we assessed the frequency of cAMP oscillations in wild-type, *adcB⁻C⁻*, and *adcB⁻C⁻* cells expressing AdcC-YFP. Cells were plated on Petri dishes containing starvation buffer to initiate development, and the aggregation stage was recorded for cAMP wave analysis. cAMP oscillations (waves) can be measured by proxy by recording optical density oscillations of cells imaged by dark-field microscopy (Siegert and Weijer, 1989; see Figure 5A). Changes in grayscale values from subregions in frame-subtracted images were measured using ImageJ. We found that wild-type cells produced waves with ~6-min period as expected (Figure 5, A and B) and displayed a robust dark-field wave pattern with broad spirals arms propagating from signaling centers (Figure 5A shows a still from the image sequence). In contrast, *adcB⁻C⁻* cells produced cAMP waves with a faster, ~3-min period (Figure 5, A and B). The shorter distance between propagating wavefronts from

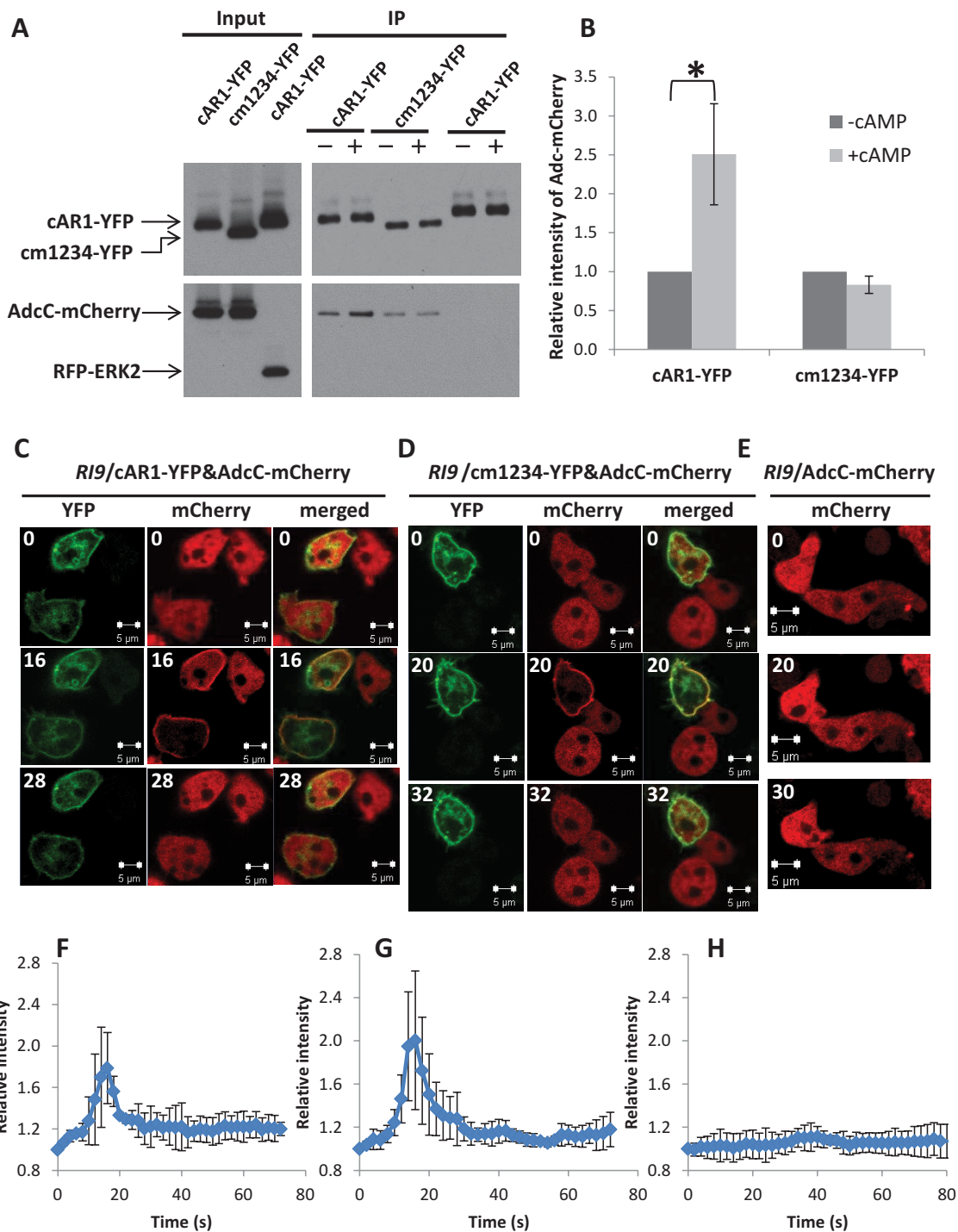


FIGURE 3: cAR1 associates with AdcC. (A, B) RI9 (*car1-/car3-*) cells coexpressing AdcC-mCherry and cAR1-YFP, AdcC-mCherry, and cm1234-YFP or RFP-ERK2 and cAR1-YFP were stimulated with 0 or 50 μ M cAMP (– or +, respectively). Membrane fractions were collected at 16 and 20 s, respectively, and lysates were incubated with beads coupled with anti-GFP antibody. Elutes were analyzed by immunoblotting using anti-GFP to detect cAR1-YFP or cm1234-YFP (top) and anti-RFP to detect AdcC-mCherry or RFP-ERK2 (bottom). Five percent of the total lysates were reserved to show input levels. Band intensities of AdcC-mCherry in A were measured by ImageJ and normalized with the amounts of cAR1-YFP or cm1234-YFP in each sample. Results represent the mean \pm SD of three independent experiments. Statistical significance was assessed by t test, * $p < 0.05$. (C–E) RI9 cells coexpressing AdcC-mCherry and cAR1-YFP (C) or cm1234-YFP (D) were stimulated with 10 μ M cAMP. Cells expressing AdcC-mCherry alone were stimulated similarly (E). Images were captured at 2-s intervals by confocal microscopy; selected time points in the YFP and mCherry channels are shown. The intensity of mCherry in the plasma membrane was measured and normalized to time 0 and is defined as 1. The kinetics of the time courses of C–E are graphed in F–H, respectively. Means ($n = 3, 4$) and SDs are shown. Scale bar, 5 μ m.

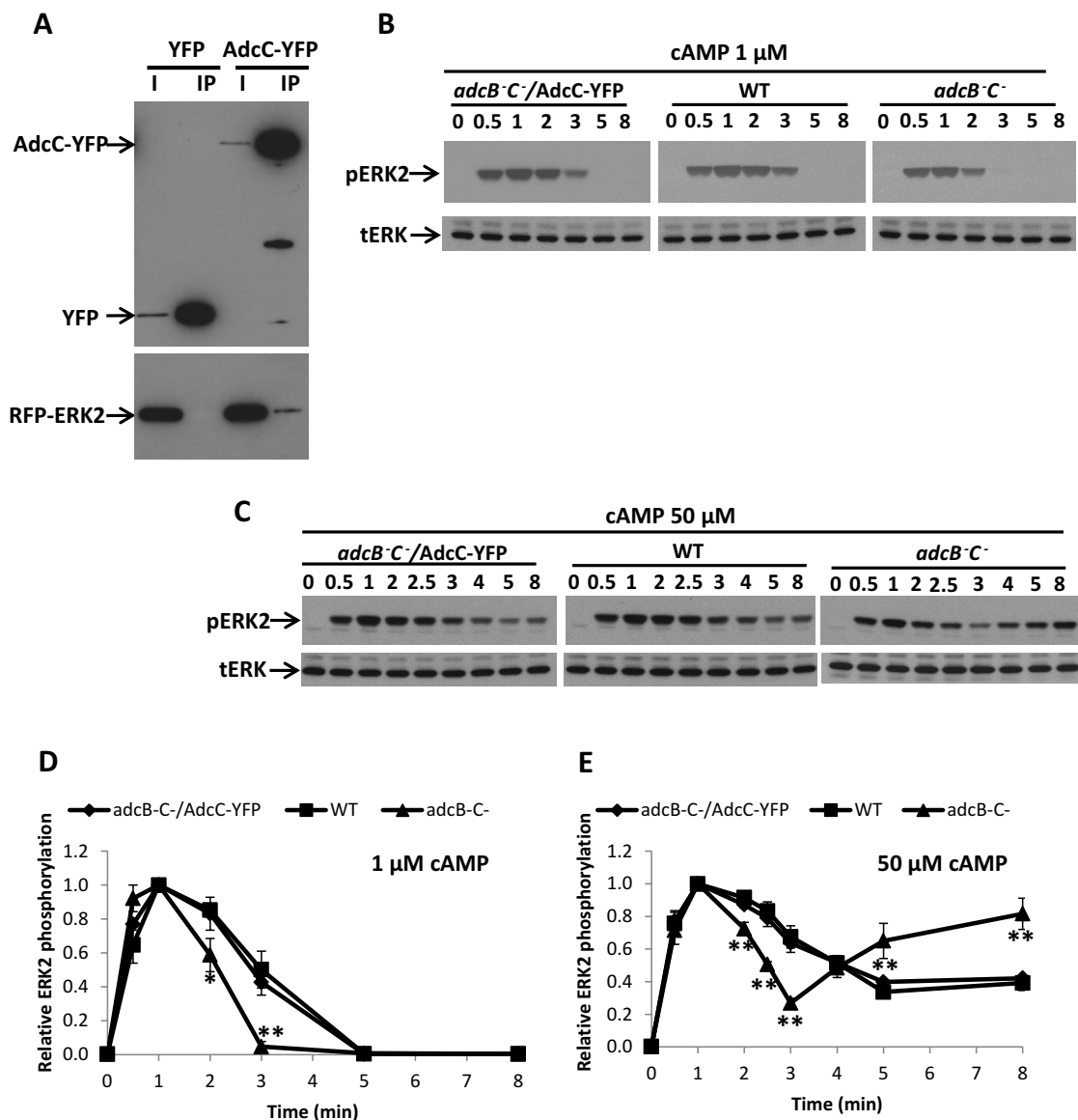


FIGURE 4: AdcC associates with ERK2 and contributes to cAMP-mediated ERK2 signaling. (A) Lysates of *adcB^{-/-}* cells coexpressing RFP-ERK2 and AdcC-YFP or YFP tag (as a control) were incubated with beads coupled with anti-GFP antibody for immunoprecipitation assays. Elutes (lane IP) were subjected to SDS gel electrophoresis and analyzed by immunoblotting using anti-GFP to detect AdcC-YFP or YFP tag (top) and anti-RFP antibody to detect RFP-ERK2 (bottom), respectively. Five percent of the total lysates were reserved to show input levels (lane I). (B, C) The kinetics of ERK2 activation in developed wild-type, *adcB^{-/-}*, and *adcB^{-/-}* cells expressing AdcC-YFP in response to a 1 or 50 μM cAMP stimulation was examined. ERK2 activation was assessed by immunoblotting with anti-phospho-ERK2 (pERK2) antibody. Western blots for total ERK (tERK) were used as loading control. The level of pERK2 was normalized to the peak value at 1 min. (D, E) The kinetics of the time course. Results represent mean ± SD of three independent experiments. Statistical significance was assessed by *t* test, ***p* < 0.01.

multiple signaling centers can be observed in the still shown in Figure 5A. Of importance, this disrupted wave pattern was rescued by expressing AdcC-YFP in the *adcB^{-/-}* cells (Figure 5, A and B). Furthermore, *adcB^{-/-}* and *adcC^{-/-}* cells did not display cAMP waves of higher frequencies (Supplemental Figure S9), suggesting that AdcB and AdcC can compensate for the loss of either one, and only in cells lacking both AdcC and AdcB is a defect in the formation of cAMP waves obvious. Our data indicate that AdcB and AdcC are involved in cAR1-mediated oscillations of cAMP signaling during the aggregation stage of *D. discoideum* development.

Arrestins are required for cAR1 internalization

β-Arrestins are well known for their roles as mediators of GPCR internalization in mammalian cells (Lefkowitz and Shenoy, 2005). To examine whether *D. discoideum* arrestins are involved in the internalization of cAR1, we expressed cAR1-YFP in wild-type or *adcB^{-/-}* cells and visualized the internalization of cAR1-YFP induced by cAMP stimulation in live cells, using confocal microscopy. We did not observe clear internalization of cAR1-YFP when cells were stimulated by <10 μM cAMP, which is the effective concentration range for cAR1-mediated cell-cell signaling and chemotaxis in the aggregation stage of development. However, we observed numerous

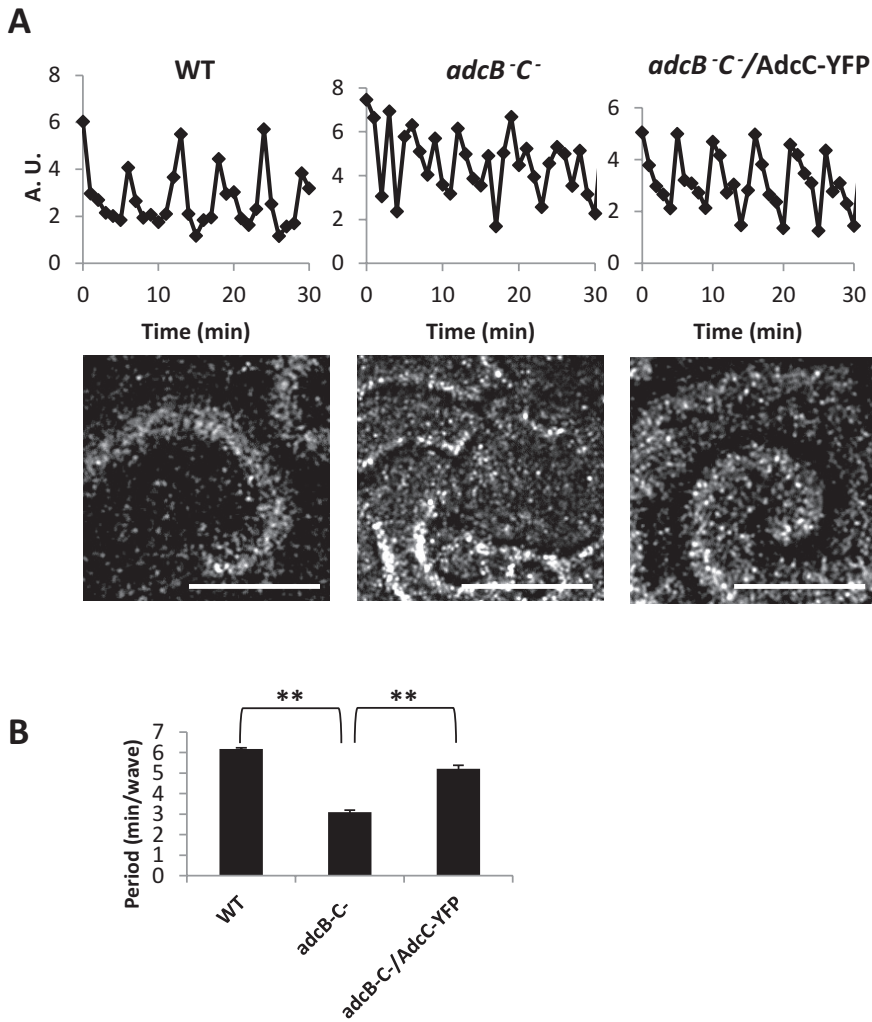


FIGURE 5: Arrestins play a role in controlling oscillations of cAMP signaling. (A) cAMP oscillations were observed in the wild-type, *adcB*^{-/-}, and *adcB*^{-/-} cells expressing AdcC-YFP during early development by capturing dark-field images every 1 min with a stereo microscope. Time plots were generated by measuring intensity changes in the frame-subtracted image sequence. Stills showing the differences in the dark-field wave patterns between the strains appear below the respective time plots. Scale bar, ~0.5 mm. (B) The period of cAMP oscillation was analyzed with three mounds per movie and graphed. Means ($n = 3$) and SDs are shown. Statistical significance was assessed by *t* test, ** $p < 0.01$. Independent experiments were performed at least twice.

intracellular vesicles containing cAR1-YFP when cells were exposed to at least 50 μM cAMP (Figure 6A). In contrast, these vesicles were not readily observed in *adcB*^{-/-} cells expressing cAR1-YFP (Figure 6A; see Supplemental Figure S10, A and B, for additional examples). To quantify internalization, we measured the ratio of intensity of YFP in the cytoplasm to that on the cell membrane and consistently found that the intracellular YFP signal was reduced in *adcB*^{-/-} cells relative to wild type after stimulation (Figure 6, A and B). We next stained cAR1-YFP-expressing cells with anti-p80 antibody. p80 is a membrane protein found throughout the endocytic pathway and accumulates on postlysosomal vacuoles (Ravel et al., 2001; Guetta et al., 2010). In wild-type cells, both proteins strongly colocalize, indicating that cAR1 is internalized via endosomes and passes through to the postlysosome compartment (Figure 6C; see Supplemental Figure S10C for additional examples). In *adcB*^{-/-} cells, cAR1-YFP did not colocalize with the p80-positive vesicle

(Supplemental Figure S11A). Finally, to determine whether receptor phosphorylation is required for cAR1 internalization, we similarly stimulated cells expressing cm1234-YFP with a high dose of cAMP and found that cm1234 did not transit to intracellular vesicles (Figure 6, D and E; see Supplemental Figure S10D for additional examples), consistent with the observation for this mutant receptor at the single-molecule level (Serge et al., 2011). In the multicellular stage of *D. discoideum* development, high-affinity cAMP receptors (cAR1s) are lost from the cell surface and replaced by low-affinity receptors, including cAR2 and cAR4, that are better suited to sense the high extracellular cAMP concentrations present in the postaggregation phase of development (Bader et al., 2007). Our results suggest that *D. discoideum* uses arrestins, AdcC and AdcB, to eliminate cAR1 receptors from the cell surface after aggregation and that the process of internalization is phosphorylation dependent. We notice that cAR1 internalization is not completely abolished by the loss of both AdcB and AdcC, and the proteins that might be responsible for the residual level of internalization need to be studied in the future.

DISCUSSION

In this study, we revealed the biological functions of AdcB and AdcC in *D. discoideum*. We discovered that AdcC plays important roles in the cAR1-controlled signaling circuit that regulates cAMP oscillations for cell-cell communication in the aggregation stage. AdcB and AdcC are necessary for cAR1 receptor internalization, which may be important for the switch to low-affinity cAMP receptors in the multicellular stages of *D. discoideum* development. Our study supports the notion that *D. discoideum* uses evolutionarily conserved arrestin-like proteins, such as AdcC, to control cell-cell signaling and GPCR internalization.

We found that cells lacking both arrestins (*adcB*^{-/-}) had a shorter period of cAMP oscillation (~3 min/wave; Figure 5, A and B), which was associated with a delay in development (Figure 1). Expressing AdcC-YFP in *adcB*^{-/-} cells restored the period of cAMP oscillations to that of wild-type cells (~6 min/wave; Figure 5, A and B) and also rescued the developmental phenotype (Figure 1). We propose that AdcC functions in cAR1-mediated signaling. Activation of cAR1 receptor regulates the function of AdcC by promoting its recruitment from the cytosol to the membrane and its association with cAR1 (Figures 2 and 3). Of interest, cAMP-induced membrane translocation of AdcC-YFP occurs in cells that have been incubated in DB (with Ca^{2+} ; see *Materials and Methods*) but not in PM buffer (Ca^{2+} free; Supplemental Figure S11B), suggesting that Ca^{2+} signaling may contribute to AdcC function upon cAMP stimulation. Future work is needed to reveal the detailed mechanism of this phenomenon. AdcC also associates with ERK2 and functions in cAR1-mediated ERK2

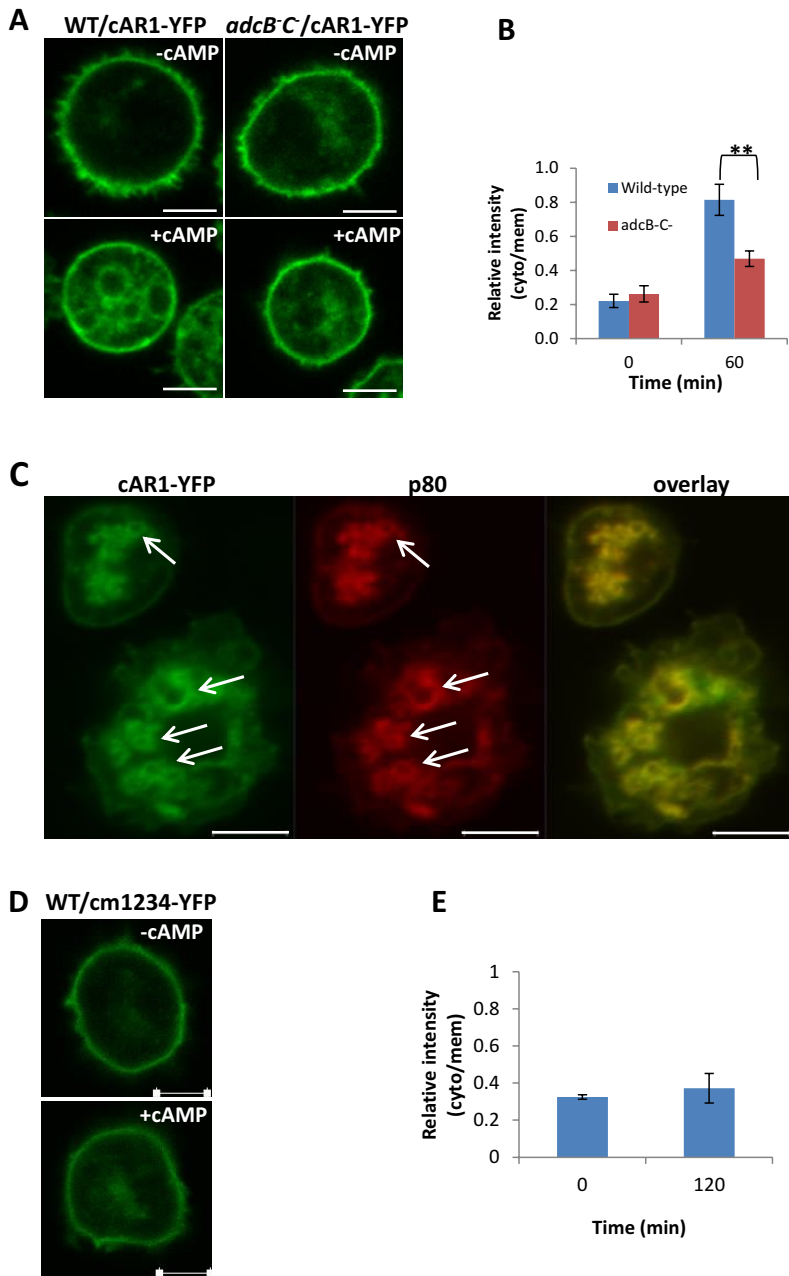


FIGURE 6: Arrestins function in cAR1 internalization. (A) Wild-type and *adcB*⁻ cells expressing cAR1-YFP were stimulated with 50 μ M cAMP. The internalization of cAR1-YFP was imaged using confocal microscopy, and photographs were taken before and 1 h after stimulation. (B) The intensity of YFP in the cytoplasm (cyto) was measured and normalized to membrane (mem) of the cells. Means ($n = 6, 7$) and SDs are shown. Statistical significance was assessed by *t* test, $**p < 0.01$. Scale bar, 5 μ m. (C) cAR1-YFP is localized on the postlysosomes after internalization. Wild-type cells expressing cAR1-YFP were stimulated with 50 μ M cAMP for 1 h, fixed, and processed for immunofluorescence assay with anti-p80. Colocalization of cAR1-YFP and p80 is indicated by arrows. Scale bar, 5 μ m. (D) cm1234 is defective in internalization. Wild-type cells expressing cm1234-YFP were stimulated with 300 μ M cAMP, and images were captured at 0 and 2 h poststimulation. (E) Intensities graphed as in B. Means ($n = 5, 6$) and SDs are shown.

signaling. Previous studies showed that activation of cAR1 not only activates ACA, which produces cAMP, but also leads to transient phosphorylation and activation of ERK2. Transient ERK activity is modulated, in part, at the level of bound cAMP ligand to cAR1 (Brzostowski and Kimmel, 2006). It was proposed that cAR1 transiently activates a kinase and persistently inhibits a phosphatase

this stage, cAR1 receptor mediates cell–cell signaling and chemotaxis when extracellular cAMP oscillates between low-nanomolar and low-micromolar concentrations levels, which cAR1 can sense without becoming saturated. After aggregation, development enters the multicellular stage. Cells in multicellular structures, such as mounds and slugs, are controlled by extracellular cAMP signaling at

(PPase) if the extracellular cAMP ligand is allowed to remain at constant levels, resulting in persistent ERK2 phosphorylation (Brzostowski and Kimmel, 2006). Thus oscillatory signaling is accomplished through the action of the extracellular cAMP-phosphodiesterase to clear the secreted cAMP for the next wave of signaling. Activated ERK2, in turn, inhibits the intracellular phosphodiesterase RegA, an enzyme that hydrolyzes cAMP (Maeda *et al.*, 2004). It has been proposed that a cAR1-mediated signaling circuit controls oscillations of both ERK2 activation and ACA activation, which leads to cAMP waves for cell–cell signaling during the development of *D. discoideum* (Maeda *et al.*, 2004). Our results showed that cAMP-triggered transient ERK2 activation occurred but with a shorter duration (~3 min) in *adcB*⁻ cells, and expressing AdcC-YFP restored the duration to that of wild-type cells (Figure 4), indicating that AdcB and AdcC are not essential for cAR1-mediated activation of ERK2 but are required for controlling the duration of transient ERK2 activity. Thus our data indicate that AdcC is likely not essential for cAR1-mediated activation of the putative ERK kinase but instead may play a role in inhibition of a PPase that regulates the duration of ERK2 activation, which, in turn, regulates RegA to maintain the frequency (~6 min) of cAMP waves in wild-type cells. Our study provides the first experimental evidence supporting the notion of the close connection between periodic ERK2 activation and frequency of cAMP waves during the aggregation stage of *D. discoideum* development. Although we postulated the involvement of kinase and phosphatase of ERK2 in the pathway, future work will be needed to identify them in *D. discoideum*, and these proposed mechanisms need to be verified in future work. Furthermore, it will be interesting to determine whether GPCR-controlled β -arrestin also functions to control oscillatory pathways in other eukaryotes and how this mechanism mediates GPCR-controlled dynamic cell–cell signaling in mammals.

Moreover, we also discovered that *D. discoideum* arrestins AdcC and AdcB, like mammalian β -arrestins (Shenoy and Lefkowitz, 2011), have a function in mediating the internalization of cAR1 GPCR. There is no clear evidence that cAR1 undergoes internalization during the aggregation stage of development (Xiao *et al.*, 1997). At

much higher concentrations (Abe and Yanagisawa, 1983; Bader et al., 2007). Consistent with these high cAMP concentrations, cells replace high-affinity cAR1s with low-affinity cAMP receptors, including cAR2 and cAR4 (Devreotes, 1994). We found that stimulation with a high dose (>50 μ M) of cAMP induced clear internalization of cAR1 receptors, and this cAMP-induced cAR1 internalization requires arrestin AdcB or AdcC (Figure 6, A and B). We also demonstrate that AdcC binds cAR1 in phosphorylation-dependent manner (Figure 3A) and show that internalization is a phosphorylation-dependent process (Figure 6, D and E), consistent with data that analyzed receptor movement at the single-molecule level (Serge et al., 2011). In addition, our data suggest that AdcC associates with *D. discoideum* homologues of clathrin and E3 ubiquitin-protein (Supplemental Figure S6B), which are evolutionarily conserved components that complex with β -arrestins to internalize ligand-bound GPCRs in mammalian cells (Krupnick et al., 1997; Shenoy et al., 2001). Taken together, our data support the notion that the simple model organism *D. discoideum* also uses arrestin-like proteins to internalize cAR1 in a phosphorylation-dependent manner to achieve cAMP receptor switching at its multicellular developmental stage. Whether arrestin-like proteins regulate internalization of other receptors will be an interesting question for future studies.

MATERIALS AND METHODS

Cell culturing and development

D. discoideum cells were grown in D3-T medium (KD Medical, Columbia, MD) to $(1-3) \times 10^6$ cells/ml and harvested by centrifugation ($400 \times g$) at 4°C for 5 min. Cells were washed in development buffer (DB; 7.4 mM $\text{NaH}_2\text{PO}_4 \cdot \text{H}_2\text{O}$, 4 mM $\text{Na}_2\text{HPO}_4 \cdot 7\text{H}_2\text{O}$, 2 mM MgCl_2 , 0.2 mM CaCl_2 , pH 6.5) twice and then resuspended in DB to 2×10^7 cells/ml. For synchronous development in shaking suspension, cells were rotated at 100 rpm on a platform shaker at 22°C and received exogenous 75 nM pulses of cAMP every 6 min. For development on lawns of *Klebsiella aerogenes*, cells were washed and resuspended in D3-T medium, mixed with bacteria, and plated on SM-agar plates without antibiotics. The plates were incubated at 22°C for 4–5 d. For development on nonnutrient agar, 5×10^6 cells were washed once with DB, plated on 1.5% agarose plates, and incubated at 22°C for 24 h after plating. Photographs were taken at indicated time points.

Generation of knock-out cells and DNA constructs

Genes were disrupted with blasticidin-resistant (BSR) cassettes between genome nucleotides 900 and 998 for *adcB*⁻ and 829 and 870 for *adcC*, respectively, by homologous recombination (Faix et al., 2004). The constructs were linearized, purified, and transfected into AX2 cells by electroporation. Transformants were selected in D3-T medium containing 10 μ g/ml blasticidin S. Individual colonies were picked from independent transformations and confirmed by PCR. To create the *adcB*⁻*C*⁻ double mutants, the plasmid pDEX-NLS-cre was transfected into *adcC*⁻ cells. The transformants were selected with 20 μ g/ml G418. Cells sensitive to both blasticidin and G418 were picked to proceed with the disruption of *adcB*⁻ as described. The final *adcB*⁻*C*⁻ double mutants were confirmed by PCR screening with primers flanking the *adcB* gene. Two independent knock-out clones for each cell line were obtained and exhibited the same phenotype.

Epitope tags were fused to the N- or C-terminus of the indicated genes and cloned into pDV-CYFP-CTAP (Veltman et al., 2009), mRFPmars (Fischer et al., 2004), or pDM326 (Veltman et al., 2009) containing the G418 or BSR cassette. Cells were transfected, and a population was selected by growing in D3-T medium containing

20 μ g/ml G418 or 10 μ g/ml blasticidin S. Constructs were confirmed by DNA sequencing. Confirmation of expression and molecular weight of the fusion proteins was performed by Western blot with indicated antibodies.

AdcC cellular distribution upon cAMP stimulation

Cells expressing AdcC-YFP or AdcC-mCherry were plated in four-well chambers (Nalge Nunc International, Naperville, IL) in 400 μ l of DB and were stimulated with 10 μ M cAMP by applying a 100- μ l volume of cAMP into the well as described previously (Xu et al., 2006, 2007). The temporal-spatial intensity changes of AdcC-YFP or AdcC-mCherry in cells were directly imaged using a Zeiss 710 or 780 LSM confocal microscope (Zeiss, Jena, Germany) using an EC plan-Neofluar objective 40 \times oil lens. To quantify the plasma membrane recruitment of YFP- or mCherry-tagged AdcC, intensities were measured using the Zeiss ZEN software package. For each cell, a region of interest (ROI) was drawn at the plasma membrane to measure the fluorescence intensity change over time. Background intensity was measured in each frame and was subtracted from the mean ROI measurements from that frame. The subtracted fluorescence intensities were normalized to the first frame with the appearance of cAMP stimulation, which is defined as 1.

Identification of proteins that interact with AdcC

Cells expressing pDV-AdcC-YFP-TAP were developed to the chemotactic stage. Cells transformed with an empty pDV-CYFP-CTAP vector were used as a control. After development with cAMP pulses, cells were washed, resuspended to 4×10^7 cells/ml in DB, and shaken with 2 mM caffeine at 200 rpm for 20 min to inhibit endogenous cAMP signaling to basal levels. Cells were then stimulated with 50 μ M cAMP, and an aliquot was removed at 16 s. Cells were lysed in lysis buffer (150 mM NaCl, 1% Triton X-100, 50 mM Tris HCl, pH 8.0) containing protease inhibitors (Roche, Chicago, IL) on ice for 30 min. Immunoprecipitation was performed by using the μ MACS GFP isolation kit (Miltenyi Biotec, Auburn, CA) according to the manufacturer's protocol. Briefly, cleared lysates were obtained by centrifugation at $10,000 \times g$ for 10 min at 4°C. Lysates were incubated with μ MACS anti-GFP MicroBeads at 4°C for 30 min. The cell lysate was then applied onto a μ Column and washed with wash buffer (150 mM NaCl, 1% Igepal CA-630, 0.5% sodium deoxycholate, 0.1% SDS, 50 mM Tris HCl, pH 8.0). Proteins were eluted with elution buffer (50 mM Tris HCl, pH 6.8, 50 mM dithiothreitol, 1% SDS, 1 mM EDTA, 0.005% bromophenol blue, 10% glycerol) and subjected to SDS-PAGE. Protein bands stained with Coomassie blue were excised for mass spectrometry analysis. Protein identification was performed using a nano liquid chromatography–tandem mass spectrometry peptide sequencing system. The mass spectrometric data acquired were analyzed by searching the most recent nonredundant protein database. A specific search was done for the *D. discoideum* database (www.dictpbase.org).

Coimmunoprecipitation

D. discoideum *adcC*⁻ cells coexpressing RFP-ERK2 and AdcC-YFP or YFP tag (as a control; 1×10^7) were stimulated with 50 μ M cAMP. Immunoprecipitations were performed by using magnetic GFP-Trap beads or RFP-Trap beads according to the manufacturer's protocol (Allele Biotech, San Diego, CA). Briefly, cells were lysed in lysis buffer (10 mM Tris HCl, pH 7.5, 150 mM NaCl, 0.5 mM EDTA, 0.5% NP40) containing protease inhibitors (Roche) on ice for 30 min. Lysates were spun at $20,000 \times g$ for 10 min at 4°C. We took 5% of cleared lysates as input control, and 95% of lysates were incubated with beads at 4°C for 30 min. The pellet was washed two times with

500 μ l of ice-cold wash buffer (10 mM Tris HCl, pH 7.5, 500 mM NaCl, 0.5 mM EDTA) and then eluted with 2 \times SDS sample buffer. The eluted proteins were separated by SDS-PAGE and probed with anti-GFP antibody (Clontech Laboratories, Mountain View, CA) or anti-RFP antibody (Allele Biotech).

To detect the association between cAR1 and AdcC, we performed coimmunoprecipitation analyses on the membrane fraction. R19 cells coexpressing mCherry-tagged AdcC and cAR1-YFP or cm1234-YFP or coexpressing RFP-tagged ERK2 and cAR1-YFP (as a negative control) were stimulated with 50 μ M cAMP. Aliquots of cells were lysed through a 5- μ m-pore polycarbonate membrane (GE Whatman, Pittsburgh, PA). Membrane fractions were collected and processed for coimmunoprecipitation as described.

cAMP oscillation assay

cAMP oscillation during self-streaming was determined as previously described (Shu *et al.*, 2010). Briefly, wild-type and *adcB*⁻ and *adcB*⁻ expressing AdcC-YFP cells were harvested and resuspended at 5 \times 10⁶/ml in HL5 medium. We plated 1.5 \times 10⁷ cells on 60-mm Petri dishes and allowed them to adhere for 30 min. The medium was then removed by aspiration, the cells were carefully washed twice with starvation buffer (20 mM 2-(N-morpholino)ethanesulfonic acid, pH 6.8, 0.2 mM CaCl₂, 2 mM MgSO₄), and 2 ml of the same buffer was applied to the plates. Aggregation and streaming were visualized up to 20 h after plating. Images of self-streaming cells were taken every minute with a Discovery V12 stereo microscope (Carl Zeiss) equipped with a PlanApos 1.0 \times objective and an AxioCam camera automated by AxioVision 4 software. The time-lapse images were subtracted, and the optical density waves were analyzed with MetaMorph software (Molecular Devices, Sunnyvale, CA).

EZ-TAXIScan chemotaxis assay

Migration of wild-type and *adcB*⁻ cells was recorded at 15-s intervals at room temperature for 30 min in an EZ-TAXIScan chamber (Effector Cell Institute, Tokyo, Japan) as described previously (Yan *et al.*, 2012). Coverslips and chips used in the chamber were coated with 1% bovine serum albumin (BSA) at room temperature for 1 h. A stable, broad cAMP gradient ranging from 0 to 1 μ M was established for the assay.

ERK2 activity assay

ERK2 phosphorylation was determined as described (Brzostowski and Kimmel, 2006). Briefly, chemotactic cells were suspended at a density of 1 \times 10⁷/ml in PB buffer (7.4 mM NaH₂PO₄·H₂O, 4 mM Na₂HPO₄·7H₂O, pH 6.5), containing 2 mM caffeine and shaken at 200 rpm for 30 min at room temperature. Cells were then washed twice with PB to remove the caffeine and resuspended at a cell density of 5 \times 10⁷ cells/ml in ice-cold PB. Before stimulation, 1.5 ml of cells was shaken at 250 rpm for 1.5 min at 20°C. Cells were stimulated with a 1:100 volume of cAMP to achieve the indicated final concentration. Then 100- μ l aliquots of cells were removed and lysed in 4 \times SDS sample buffer (Invitrogen, Carlsbad, CA) at selected times. Protein was separated by SDS-PAGE, transferred to nitrocellulose membranes, and blotted with polyclonal anti-phospho-p44/p42 MAPK (pERK2) antibody (Cell Signaling Technology, Beverly, MA).

Internalization of the cAR1

Wild-type and *adcB*⁻ cells expressing cAR1-YFP or cAR1cm1234-YFP were plated in four-well chambers (Nalge Nunc International) in 400 μ l of DB. The cells were stimulated at the indicated dose of cAMP by applying a 100- μ l volume of cAMP into the well.

The internalization of cAR1-YFP was imaged using a Zeiss 710 or 780 LSM confocal microscope using an EC plan-Neofluar 40 \times oil lens. Photographs were taken after 1 h. The internalization was assessed by normalizing the intensity of YFP in the cytoplasm to the membrane of the cells.

Immunofluorescence assay

Immunofluorescence assays were performed as described (Shu *et al.*, 2012). Briefly, cells expressing cAR1-YFP were placed on a two-well chamber (Nalge Nunc International) in DB and treated with 50 μ M cAMP for 1 h. Cells were fixed with 1% formaldehyde, 0.1% glutaraldehyde, and 0.01% Triton X-100 in phosphate buffer (PB; 5 mM Na₂HPO₄, 5 mM KH₂PO₄, pH 6.2) at room temperature for 15 min, washed with phosphate buffer, and incubated with monoclonal mouse anti-p80 endosomal membrane protein antibody (Developmental Studies Hybridoma Bank, University of Iowa, Iowa City, IA) for 60 min at 37°C with 20-fold dilution. Cells were then washed and incubated with secondary antibody Alexa Fluor 532 goat anti-mouse immunoglobulin G (Life Technologies, Grand Island, NY) with 700-fold dilution. Antibodies were diluted in phosphate buffer supplemented with 1% BSA and 0.2% saponin. Images were acquired with a Zeiss 780 LSM equipped with an EC plan-Neofluar 40 \times oil lens.

ACKNOWLEDGMENTS

This study was supported by the Intramural Research Program of the National Institute of Allergy and Infectious Diseases/National Institutes of Health and grants from the National Basic Research Program of China (2014CB541804) and the Shanghai Pujiang Program (14PJ1407700). The plasmids pLPBLP, pDEX-NLS-cre, pDV-CYFP-CTAP, pDM326, and pDXA-MCS-YFP were obtained through the Dicty Stock Center (<http://dictybase.org/>). We thank A. Muller-Taubenberger (Ludwig Maximilians University of Munich, Munich, Germany) for providing the mRFPmars plasmid. We are appreciative to X. Xiang (Uniformed Services University of the Health Sciences, Bethesda, MD) and D. Hereld (National Institute on Alcohol Abuse and Alcoholism, Bethesda, MD) for insightful discussions and comments. We also thank E. Korn and X. Liu (National Heart, Lung, and Blood Institute, Bethesda, MD), X. Xu and M. Zhao (National Institute of Allergy and Infectious Diseases, Bethesda, MD), and Y. Yuan, H. Liu, and Y. Hou (Shanghai Jiao Tong University School of Medicine, Shanghai, China) for their generous assistance.

REFERENCES

- Abe K, Yanagisawa K (1983). A new class of rapidly developing mutants in *Dictyostelium discoideum*: implications for cyclic AMP metabolism and cell differentiation. *Dev Biol* 95, 200–210.
- Alvarez CE (2008). On the origins of arrestin and rhodopsin. *BMC Evol Biol* 8, 222.
- Aubry L, Guetta D, Klein G (2009). The arrestin fold: variations on a theme. *Curr Genomics* 10, 133–142.
- Bader S, Kortholt A, Van Haastert PJ (2007). Seven *Dictyostelium discoideum* phosphodiesterases degrade three pools of cAMP and cGMP. *Biochem J* 402, 153–161.
- Brzostowski JA, Kimmel AR (2001). Signaling at zero G: G-protein-independent functions for 7-TM receptors. *Trends Biochem Sci* 26, 291–297.
- Brzostowski JA, Kimmel AR (2006). Nonadaptive regulation of ERK2 in *Dictyostelium*: implications for mechanisms of cAMP relay. *Mol Biol Cell* 17, 4220–4227.
- DeFea KA (2007). Stop that cell! Beta-arrestin-dependent chemotaxis: a tale of localized actin assembly and receptor desensitization. *Annu Rev Physiol* 69, 535–560.

- DeFea KA (2011). Beta-arrestins as regulators of signal termination and transduction: how do they determine what to scaffold? *Cell Signal* 23, 621–629.
- Devreotes PN (1994). G protein-linked signaling pathways control the developmental program of Dictyostelium. *Neuron* 12, 235–241.
- Faix J, Kreppel L, Shaulsky G, Schleicher M, Kimmel AR (2004). A rapid and efficient method to generate multiple gene disruptions in Dictyostelium discoideum using a single selectable marker and the Cre-loxP system. *Nucleic Acids Res* 32, e143.
- Fischer M, Haase I, Simmeth E, Gerisch G, Muller-Taubenberger A (2004). A brilliant monomeric red fluorescent protein to visualize cytoskeleton dynamics in Dictyostelium. *FEBS Lett* 577, 227–232.
- Funamoto S, Meili R, Lee S, Parry L, Firtel RA (2002). Spatial and temporal regulation of 3-phosphoinositides by PI 3-kinase and PTEN mediates chemotaxis. *Cell* 109, 611–623.
- Funamoto S, Milan K, Meili R, Firtel RA (2001). Role of phosphatidylinositol 3' kinase and a downstream pleckstrin homology domain-containing protein in controlling chemotaxis in dictyostelium. *J Cell Biol* 153, 795–810.
- Gerisch G, Hulser D, Malchow D, Wick U (1975). Cell communication by periodic cyclic-AMP pulses. *Philos Trans R Soc Lond B Biol Sci* 272, 181–192.
- Goldbeter A (2002). Computational approaches to cellular rhythms. *Nature* 420, 238–245.
- Granier S, Kim S, Shafer AM, Ratnala VR, Fung JJ, Zare RN, Kobilka B (2007). Structure and conformational changes in the C-terminal domain of the beta2-adrenoceptor: insights from fluorescence resonance energy transfer studies. *J Biol Chem* 282, 13895–13905.
- Gregor T, Fujimoto K, Masaki N, Sawai S (2010). The onset of collective behavior in social amoebae. *Science* 328, 1021–1025.
- Guetta D, Langou K, Grunwald D, Klein G, Aubry L (2010). FYVE-dependent endosomal targeting of an arrestin-related protein in amoeba. *PLoS One* 5, e15249.
- Gutkind JS (2000). Regulation of mitogen-activated protein kinase signaling networks by G protein-coupled receptors. *Sci STKE* 2000, re1.
- Hereld D, Vaughan R, Kim JY, Borleis J, Devreotes P (1994). Localization of ligand-induced phosphorylation sites to serine clusters in the C-terminal domain of the Dictyostelium cAMP receptor, cAR1. *J Biol Chem* 269, 7036–7044.
- Iijima M, Devreotes P (2002). Tumor suppressor PTEN mediates sensing of chemoattractant gradients. *Cell* 109, 599–610.
- Insall RH, Soede RD, Schaap P, Devreotes PN (1994). Two cAMP receptors activate common signaling pathways in Dictyostelium. *Mol Biol Cell* 5, 703–711.
- Janetopoulos C, Jin T, Devreotes P (2001). Receptor-mediated activation of heterotrimeric G-proteins in living cells. *Science* 291, 2408–2411.
- Klein P, Vaughan R, Borleis J, Devreotes P (1987). The surface cyclic AMP receptor in Dictyostelium. Levels of ligand-induced phosphorylation, solubilization, identification of primary transcript, and developmental regulation of expression. *J Biol Chem* 262, 358–364.
- Kosaka C, Pears CJ (1997). Chemoattractants induce tyrosine phosphorylation of ERK2 in Dictyostelium discoideum by diverse signalling pathways. *Biochem J* 324, 347–352.
- Kriebel PW, Barr VA, Parent CA (2003). Adenylyl cyclase localization regulates streaming during chemotaxis. *Cell* 112, 549–560.
- Krupnick JG, Goodman OB Jr, Keen JH, Benovic JL (1997). Arrestin/clathrin interaction. Localization of the clathrin binding domain of nonvisual arrestins to the carboxy terminus. *J Biol Chem* 272, 15011–15016.
- Lefkowitz RJ, Shenoy SK (2005). Transduction of receptor signals by beta-arrestins. *Science* 308, 512–517.
- Lohse MJ, Benovic JL, Codina J, Caron MG, Lefkowitz RJ (1990). beta-Arrestin: a protein that regulates beta-adrenergic receptor function. *Science* 248, 1547–1550.
- Maeda M, Aubry L, Insall R, Gaskins C, Devreotes PN, Firtel RA (1996). Seven helix chemoattractant receptors transiently stimulate mitogen-activated protein kinase in Dictyostelium. Role of heterotrimeric G proteins. *J Biol Chem* 271, 3351–3354.
- Maeda M, Lu S, Shaulsky G, Miyazaki Y, Kuwayama H, Tanaka Y, Kuspa A, Loomis WF (2004). Periodic signaling controlled by an oscillatory circuit that includes protein kinases ERK2 and PKA. *Science* 304, 875–878.
- Parent CA, Blacklock BJ, Froehlich WM, Murphy DB, Devreotes PN (1998). G protein signaling events are activated at the leading edge of chemotactic cells. *Cell* 95, 81–91.
- Parent CA, Devreotes PN (1996). Molecular genetics of signal transduction in Dictyostelium. *Annu Rev Biochem* 65, 411–440.
- Ravanel K, de Chasse B, Cornillon S, Benghezal M, Zulianello L, Gebbie L, Letourneur F, Cosson P (2001). Membrane sorting in the endocytic and phagocytic pathway of Dictyostelium discoideum. *Eur J Cell Biol* 80, 754–764.
- Sasaki AT, Chun C, Takeda K, Firtel RA (2004). Localized Ras signaling at the leading edge regulates PI3K, cell polarity, and directional cell movement. *J Cell Biol* 167, 505–518.
- Segall JE, Kuspa A, Shaulsky G, Ecke M, Maeda M, Gaskins C, Firtel RA, Loomis WF (1995). A MAP kinase necessary for receptor-mediated activation of adenylyl cyclase in Dictyostelium. *J Cell Biol* 128, 405–413.
- Serge A, de Keijzer S, Van Hemert F, Hickman MR, Hereld D, Spaink HP, Schmidt T, Snaar-Jagalska BE (2011). Quantification of GPCR internalization by single-molecule microscopy in living cells. *Integr Biol (Camb)* 3, 675–683.
- Shenoy SK, Lefkowitz RJ (2011). beta-Arrestin-mediated receptor trafficking and signal transduction. *Trends Pharmacol Sci* 32, 521–533.
- Shenoy SK, McDonald PH, Kohout TA, Lefkowitz RJ (2001). Regulation of receptor fate by ubiquitination of activated beta 2-adrenergic receptor and beta-arrestin. *Science* 294, 1307–1313.
- Shukla AK, Manglik A, Kruse AC, Xiao K, Reis RI, Tseng WC, Staus DP, Hilger D, Uysal S, Huang LY, et al. (2013). Structure of active beta-arrestin-1 bound to a G-protein-coupled receptor phosphopeptide. *Nature* 497, 137–141.
- Shu S, Liu X, Kriebel PW, Daniels MP, Korn ED (2012). Actin cross-linking proteins cortexillin I and II are required for cAMP signaling during Dictyostelium chemotaxis and development. *Mol Biol Cell* 23, 390–400.
- Shu S, Liu X, Kriebel PW, Hong MS, Daniels MP, Parent CA, Korn ED (2010). Expression of Y53A-actin in Dictyostelium disrupts the cytoskeleton and inhibits intracellular and intercellular chemotactic signaling. *J Biol Chem* 285, 27713–27725.
- Siegert F, Weijer C (1989). Digital image processing of optical density wave propagation in Dictyostelium discoideum and analysis of the effects of caffeine and ammonia. *J Cell Sci* 93, 325–335.
- Tomchik KJ, Devreotes PN (1981). Adenosine 3',5'-monophosphate waves in Dictyostelium discoideum: a demonstration by isotope dilution-fluorography. *Science* 212, 443–446.
- Veltman DM, Akar G, Bosgraaf L, Van Haastert PJ (2009). A new set of small, extrachromosomal expression vectors for Dictyostelium discoideum. *Plasmid* 61, 110–118.
- Xiao Z, Zhang N, Murphy DB, Devreotes PN (1997). Dynamic distribution of chemoattractant receptors in living cells during chemotaxis and persistent stimulation. *J Cell Biol* 139, 365–374.
- Xu X, Brzostowski JA, Jin T (2006). Using quantitative fluorescence microscopy and FRET imaging to measure spatiotemporal signaling events in single living cells. *Methods Mol Biol* 346, 281–296.
- Xu X, Meier-Schellersheim M, Jiao X, Nelson LE, Jin T (2005). Quantitative imaging of single live cells reveals spatiotemporal dynamics of multistep signaling events of chemoattractant gradient sensing in Dictyostelium. *Mol Biol Cell* 16, 676–688.
- Xu X, Meier-Schellersheim M, Yan J, Jin T (2007). Locally controlled inhibitory mechanisms are involved in eukaryotic GPCR-mediated chemosensing. *J Cell Biol* 178, 141–153.
- Yan J, Mihaylov V, Xu X, Brzostowski JA, Li H, Liu L, Veenstra TD, Parent CA, Jin T (2012). A Gbetagamma effector, ElmoE, transduces GPCR signaling to the actin network during chemotaxis. *Dev Cell* 22, 92–103.